NJC

Accepted Manuscript

This is an *Accepted Manuscript*, which has been through the Royal Society of Chemistry peer review process and has been accepted for publication.

Accepted Manuscripts are published online shortly after acceptance, before technical editing, formatting and proof reading. Using this free service, authors can make their results available to the community, in citable form, before we publish the edited article. We will replace this *Accepted Manuscript* with the edited and formatted *Advance Article* as soon as it is available.

You can find more information about *Accepted Manuscripts* in the Information for Authors.

Please note that technical editing may introduce minor changes to the text and/or graphics, which may alter content. The journal's standard Terms & Conditions and the Ethical guidelines still apply. In no event shall the Royal Society of Chemistry be held responsible for any errors or omissions in this *Accepted Manuscript* or any consequences arising from the use of any information it contains.

ROYAL SOCIETY OF CHEMISTRY

www.rsc.org/njc

NJC

RSCPublishing

Article

Supramolecular self-assembly of 14-helical nanorods with tunable linear and dendritic hierarchical morphologies

Cite this: DOI: 10.1039/c3nj00000x

Received 00thXXXXX 2013,
Accepted 00thXXXXX 2013

DOI: 10.1039/c3nj00000x

www.rsc.org/njc

Rania S. Seoudi[a], Mark P. Del Borgo[b], Ketav Kulkarni[c], Patrick Perlmutter[c], Marie-Isabel Aguilar[b], and Adam Mechler*[a]

*Corresponding author. E-mail: a.mechler@latrobe.edu.au

Bioinspired self-assembly offers a way to create novel functional materials from simple, easy-to-synthesize building blocks. Peptides, in particular, are frequently used in the design of self-assembled materials for their structural properties and the ability for supramolecular "lock and key" type recognition based on H-bonding networks and dispersion interactions. We have previously reported the head-to-tail self-assembly of N-terminal acetylated β-peptides into helical fibrils through a supramolecular three point H-bonding motif, and the superstructures formed from inter-fibril interactions. Here we show that the superstructure morphology of a self-assembled β^3-peptide, Ac-β^3[LIA], can be tuned to present a range of morphologies by the appropriate solvent medium. From the same monomer we succeeded in creating straight compact "nano-beams", self-spun threads and complex, dendritic, hierarchical structures. The variation in geometries is therefore achieved through careful switching and tuning of the relative strengths of the inter-fibril H-bonding, van der Waals and solvophobic interactions.

Introduction

Peptide self-assembly offers a versatile platform for developing novel functional nanomaterials[1, 2, 3]. Peptides are biocompatible[4], easy to synthesize and functionalize[3], and fold into known structures controlled by the amino acid sequence[5], allowing the design of self-assembling systems of specific geometries, e.g. fibres[6, 7], nano-tubes[8] and nano-tapes[9]. However, precise control of structure and function is a significant challenge but essential for several target applications including tissue engineering[10], regenerative medicine[11] and drug delivery[12]. It is particularly difficult to design hierarchical materials, assemblies made of structural elements which themselves have distinct structures on multiple levels of scale.[13]
In a recent study we described the design of helical *N*-acetyl-β^3-peptides that spontaneously self-assemble into nano- to macro-scale fibres. The peptide monomers bind in a unique head-to-tail fashion driven by a 3-point H-bond motif associated with the 14-helical structure of *N*-acetyl-β^3-peptides, providing controlled alignment of side chains due to a near perfect pitch of three residues per turn[1,14]. These fibrils further associate laterally through interactions between the side chains to form hierarchical macrostructures, creating a unique platform for the design of smart materials *via* chemical modification of the amino acid side chains or *via* manipulation of the intermolecular H-bonding and van der Waals (VdW) interactions. [14,15,16]
In this study, we sought to control the superstructure geometry of the *N*-acetyl-β^3-peptide fibres *via* controlling the lateral interactions between the nanorods[6, 17,18]. The peptide sequence Ac-β^3[LIA] (Figure 1a) is neutral in pure solvents, thus electrostatic interactions do not play a role in the lateral fibre assembly, leaving only second order interactions that are generally sensitive to environmental factors[19,20]. This offers the unique opportunity to tune the morphology of Ac-β^3[LIA] superstructures *via* changing the solvent.
The strength of VdW and H-bonding is inversely proportional to the dielectric constant of the medium[19, 21]. The relative energies of the H-bonding interactions between peptide-peptide, peptide-solvent and solvent-solvent also vary with solvent and changing the relative contribution of these forces can affect peptide self-assembly. In protic solvents the solvophobic effect exerts an attractive force between apolar solutes[22], the magnitude of which is dependent on the strength of the H-bonding between solvent molecules[19]. Furthermore, H-bonding between fibres enhances the specificity of self-

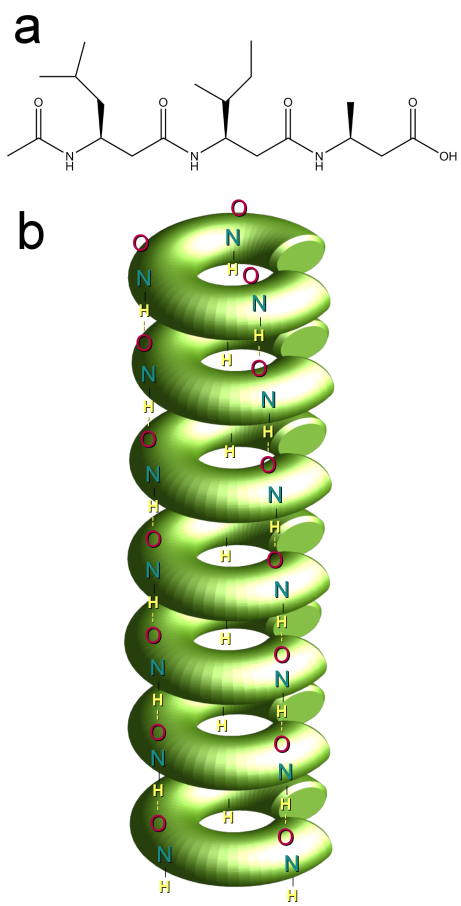

Figure 1: a, The molecular structure of Ac-β[3][LIA]. b, Schematics of the helical nanorod that is the primary self-assembled structure of the N-acyl β[3] peptides. N-acyl tri-β[3] peptide monomers are symbolized by the green tori; the three point H-bonding self-assembly motif is indicated with the appropriate atomic symbols.

assembly[23] and thus competition from solvent molecules for the H-bonding sites may alter the resulting structure. Accordingly, if two fibres interact with a combination of VdW, H-bonding and solvophobic attraction, changing the solvent offers a simple way to control the dominance of one of the three forces and thus the geometry of the self-assembled superstructure. For example, using methanol instead of water would weaken, but not eliminate, hydrophobic interactions, while at the same time allowing stronger VdW interactions due to its lower dielectric constant [24]. Since second order interactions can be overcome by the Boltzmann energy (kT) at temperatures below 100°C, changing the temperature can also change the morphology of self-assembled materials.[25]

In this study we have exploited the sensitivity of second order interactions to solvent and temperature to tune superstructure morphology of Ac-β[3][LIA] with the aim of designing hierarchical materials.

Results

Strategy to control interactions in self-assembled Ac-β3[LIA]

Figure 1a illustrates the primary self-assembly motif of Ac-β[3][LIA]: the three-point supramolecular H-bonding network that forms an extended 14-helix fibril (nanorod)[1]. The strength of this motif allows only limited manipulation of the longitudinal self-assembly process through solvent competition for the H-bonding sites. However, the lateral interactions between the fibrils are amenable to significant modulation. The fibrils interact with a combination of hydrophobic attraction, VdW interaction between the amino acid side chains, and potentially inter-fibril H-bonding from the exposed C-terminal carboxyl groups, which are also the most hydrophilic parts of the peptide. These interactions are strongly solvent dependent and their relative strengths and topographic distribution between neighbouring fibrils dominate lateral assembly, resulting in a solvent-dependent hierarchical structure.

In order to control the rate and geometry of self-assembly, three effects have to be considered: 1) the strength of interaction between solvent and peptide molecules, which affects solubility and the kinetics of self-assembly; 2) the dielectric constant of the medium that affects the VdW interaction between the fibres, and also influences the strength of the supramolecular H-bonds; and 3) solvation effects (such as hydrophobicity). We therefore investigated the effect of a range of solvents on the morphology of materials obtained from the self-assembly of Ac-β[3][LIA]. Protic solvents with a range of H-bonding strength and dielectric constants were selected for their ability to compete for H-bonding during fibril self-assembly and to exert variable solvophobic effects. Acetone was selected as a non-protic polar solvent, while chloroform was used as a representative apolar solvent to eliminate the "hydrophobic" component of inter-fibril interactions while maximising the strength of

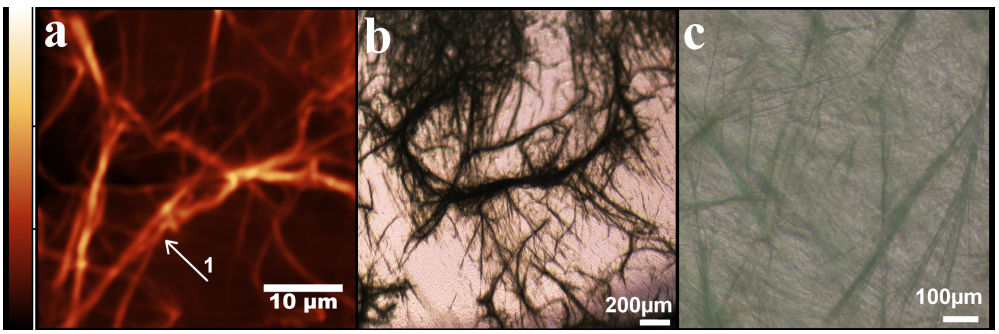

Figure 2: Images of Ac-β[3][LIA] structures deposited from water. a, AFM image; size 40X40μm, height scale 0.6μm. b, optical microscopy image of a deposit. c, optical microscopy image of mesh formed upon heating the aqueous suspension.

supramolecular (and inter-fibril) H-bonding

Water induces the formation of rope-like twisted hierarchical structures

The largely hydrophobic Ac-β[3][LIA] dissolved easily in water. Optical microscopy imaging revealed a few large fibres immediately following dissolution, however no more fibres formed upon aging for several days. AFM images of the deposits of these solutions, however, showed fibre bundles (arrow no. 1 Figure 2a) of tens to hundreds of nm in thickness and of considerable length (Figure 2a). These fibres were mostly straight, showing a twisted rope-like hierarchical structure. It appears that the fibres formed pre-deposition as several of the fibres lay across the top of other fibres. Since fibres were not visible *via* optical microscopy, it is likely that only small, colloidal fibres formed in solution. Assuming that fibre growth is hindered by H-bonding of water to the peptides, heat treatment was used to weaken peptide-water interaction and increase fibre formation. Heating the solution to 75°C accelerated fibre growth, and led to the formation of masses of fibres that ascended to the surface of the solvent to form an irregular mesh (Figure 2c)

Alcohols induce the formation of dendritic hierarchical structures

Methanol dissolution of Ac-β[3][LIA] resulted in the reproducible formation of fibres observable by optical microscopy, as reported previously[1]. However, drop-casting the solution at room temperature onto an atomically smooth mica surface only occasionally yielded discernible fibrous nanostructures, the primary morphology being amorphous shapes as observed by AFM (Figure 3a). This suggests that the solution did not contain a significant amount of nano-fibres, but rather monomeric peptide or small aggregates co-existing with large fibres of several 100 micrometer dimensions that were observable by optical microscopy but too large for AFM imaging. The deposit also exerted much higher adhesion on the probe than bare mica, suggesting that it was a largely fluid layer with sufficient plasticity and surface tension to generate strong meniscus forces. The deposit was therefore likely to be a mixture of monomers and/or small oligomers with residual methanol. Drying the sample under nitrogen and aging for 2 hours at 37°C reduced adhesion, indicating that the deposit was capable of some degree of rearrangement, most likely loss of solvent, however post deposition fibre formation was not observed. In contrast, the deposits from an aged (more than one month old) solution showed none of the amorphous structures, instead revealing bundles of small fibres(arrow no.1 Figure 3b) similar to the structures observed in case of water, as well as robust, ribbon-like structures (arrow no.2 Figure 3b), similar to those observed under the optical microscope, suggesting that these fibres were formed in solution with slow kinetics (Figure

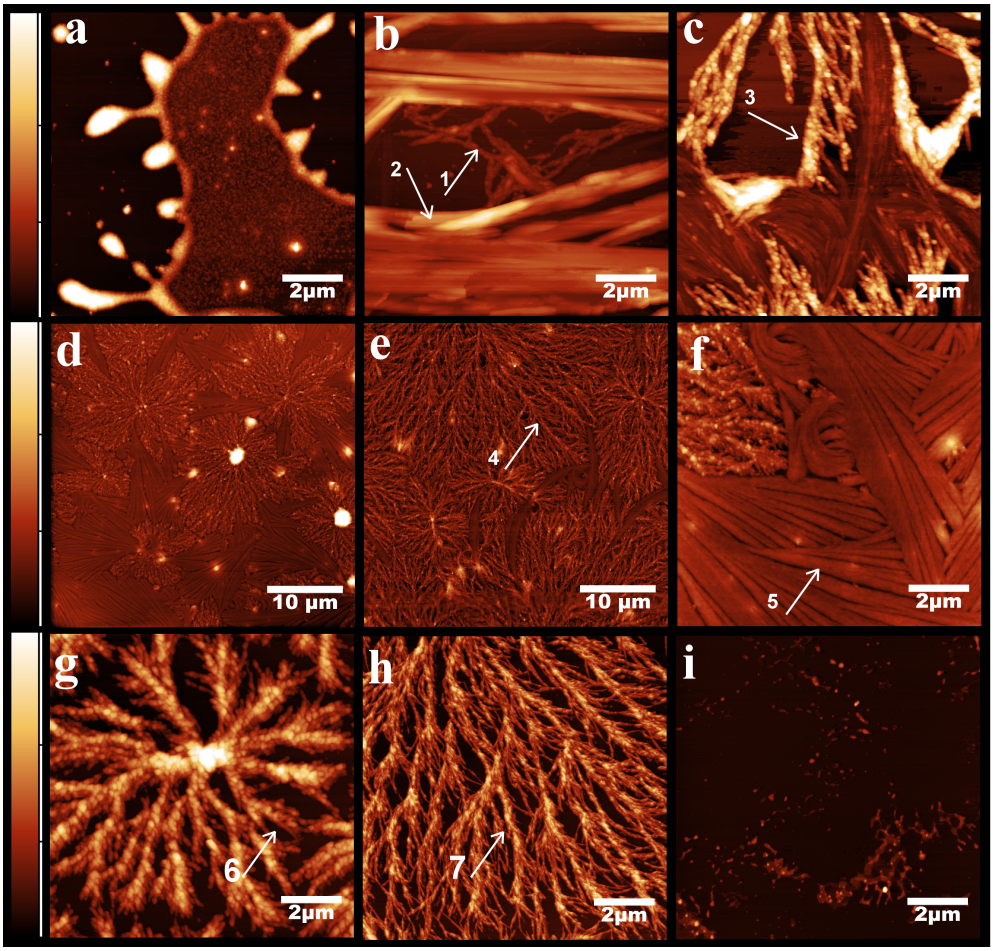

Figure 3: AFM images of Ac-β[3][LIA] structures deposited from various alcohols. a, deposit of fresh methanol solution; b, deposit of aged methanol solution; c, deposited from methanol, after further addition of isopropanol solvent. Height scales 36nm, 159.2nm and 53.9nm, respectively. d-f AFM images of Ac-β[3][LIA] deposited from ethanol, height scales 120nm, 114.9nm and 60nm, respectively. d shows structures formed at 37°C; e shows structures formed at room temperature; f a zoom on the ribbon structures from (e). g-i, AFM image of Ac-β[3][LIA] deposited from isopropanol, height scales 74.3nm, 51.9nm and 54.5nm, respectively. At 37°C the average diameter of the dendritic structures was ~ 9.6 µm (g); at room temperature the average diameter of the dendritic structure was ~27.3µm (h); dendritic structures disappear after a wash with methanol (i).

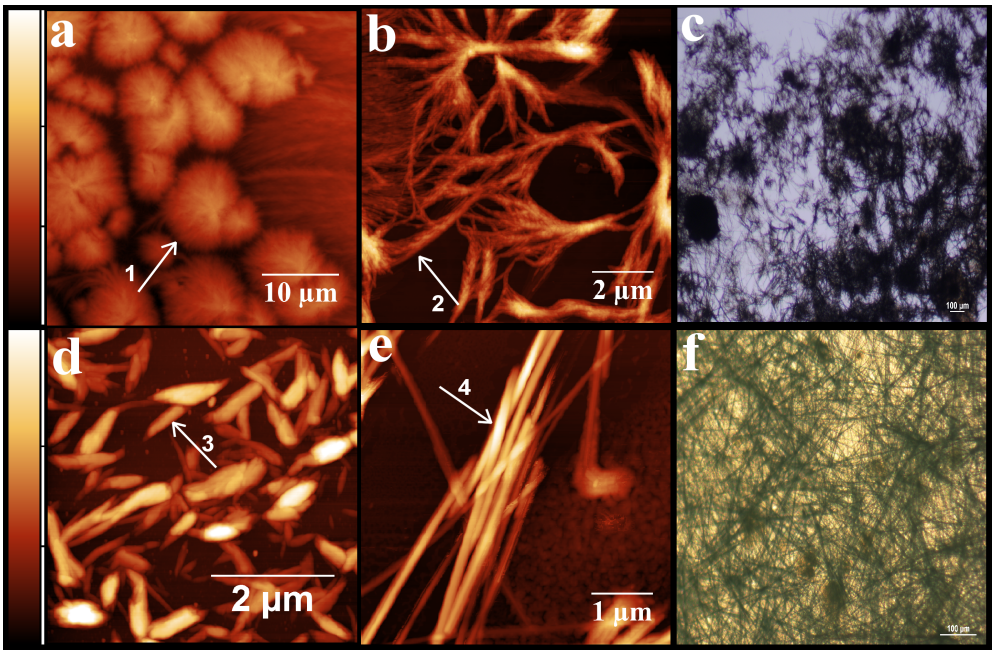

Figure 4: Images of Ac-β[3][LIA] deposited from non-protic solvents. a-b, AFM images of deposits from acetone, height scales 83.2nm and 1.0µm, respectively. c, optical microscopy image of Ac-β[3][LIA] deposited from acetone, scale bar 100µm. d-e, AFM images of Ac-β[3][LIA] deposit from chloroform, height scales 43nm and 158.1nm, respectively; (e) is further diluted with chloroform before deposition. f, optical microscopy image of Ac-β[3][LIA] deposited from chloroform, scale bar 100µm.

3b).

Ethanol also fully dissolved the lyophilised peptide. The deposits contained a combination of flat, straight ribbons (arrow no.5 Figure 3f) and hierarchical dendritic structures formed by twisting of nanorods into fibres (arrow no.4; Figure 3e) which then further coiled into larger "ropes" towards the centre of the structure (Figure 3 d,e). The proportion of flat ribbons was higher in samples annealed at 37°C (Figure 3d, f, arrow no.6) compared to room temperature (Figure 3e; arrow no.7).

In isopropanol, fibre nucleation was observed in bulk solution soon after peptide dissolution.Deposits on mica surface contained only dendritic fibrous structures (Figure 3 g,h). However, the size and nucleation density of the structures were influenced by the annealing temperature. At 37°C the average diameter of the structures was ~ 9.6 µm (Figure 3g), with a proportionally higher nucleation density than the structures grown at room temperature (Figure 3h) which had an average diameter of ~27.3µm. Assuming a negligible gap between the structures, the surface density was ~14000 structure/mm^2 and ~1700 structure/mm^2 for 37°C and room temperature, respectively.

When a drop of isopropanol was added onto an amorphous deposit formed from methanol (Figure 3c), fast fibre formation was observed with mixed morphologies dominated by dendritic hierarchical structures and a few flat ribbon structures. Isopropanol therefore facilitates post-deposition fibre formation. When the opposite experiment was performed by adding methanol to the dendritic deposit, the structures were washed away (Figure 3i). The relatively weak surface adhesion implies that dendritic fibre growth is aided, but not templated by the surface

Acetone causes the formation of spherical "urchin" structures

Acetone is a polar solvent that can act as a H-bond acceptor *via* the ketone oxygen but does not cause a solvophobic effect. AFM images (Figure 4a,b) show dense micelle-like (arrow no.1 Figure 4a) structures consisting of straight, mostly short fibres growing from a centre without branching(arrow no.2 Figure 4b). Temperature variations did not lead to noticeable differences in the fibre structures.

Chloroform induces the formation of straight fibres

Chloroform is a non-H-bonding apolar solvent. Deposition of the sample at room temperature yielded straight but generally short fibres(arrow no.3; Figure 4d) with varied thickness (Figure 4d) but occasionally large rods (arrow no.4; Figure 4e) of rectangular cross section and micron dimensions, with lengths too large for AFM imaging (Figure 4e). Changes in temperature had no effect on fibre morphology.

The abundance of the fibres suggests that the chloroform promotes self-assembly because it does not compete with the longitudinal intramolecular peptide hydrogen bonds. Considering the high vapour pressure, and thus fast drying of chloroform, the large fibres observed on the surface also most likely formed in solution prior to deposition. The chloroform solution also yielded floating cottonwool-like structures as seen under the optical microscope that could not be imaged

Discussion

Solvation requirements for controlled self-assembly

The aim of this study was to control the lateral interaction, and thus the superstructure morphology of the self-assembled peptide helices (nanorods) by varying the solvents used for deposition, thereby creating hierarchical structures. Controlled

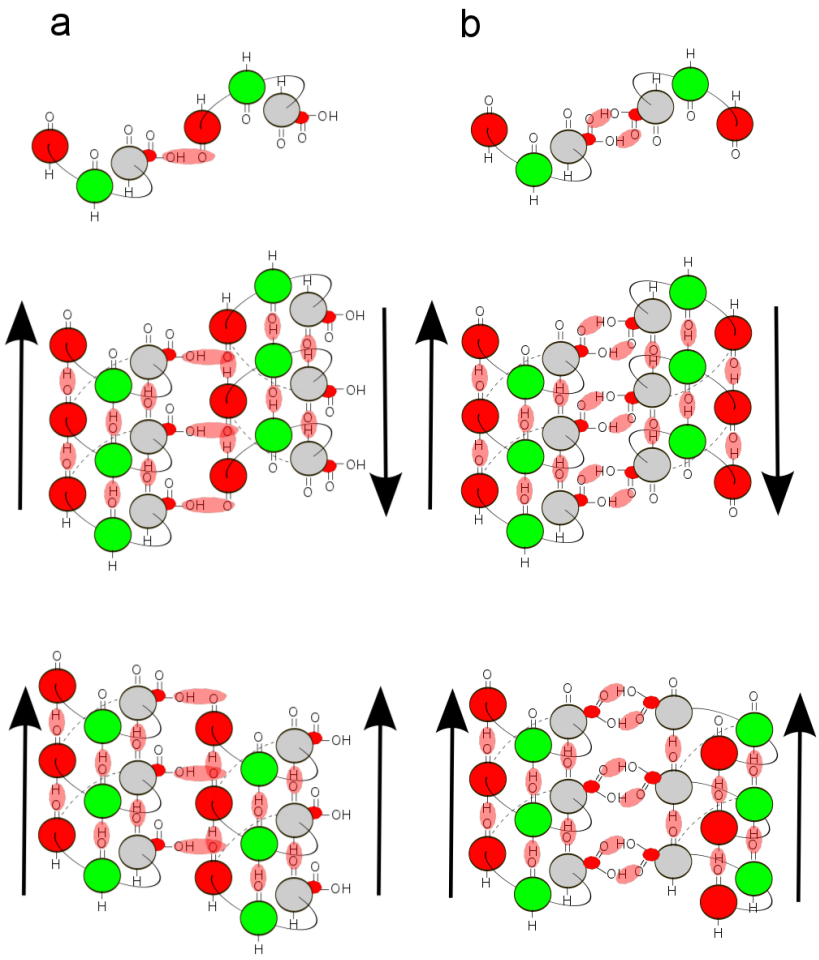

Figure 5: Possibilities for inter-fibril H-bonding. a, carboxyl dimerization, parallel and antiparallel; b, secondary H-bonding to carbonyl oxygen, parallel and antiparallel.

self-assembly requires a medium that 1) solvates peptide monomers, 2) slows down nucleation without preventing fiber growth at higher concentrations, 3) provides the mobility needed for the peptides to find the termini of existing fibres, 4) controls inter-fibril H-bonding, and 5) modulates strong solvophobic attraction between the fibrils. Common solvents succeed to different degrees in meeting these requirements, and in the present study their use resulted in a range of different superstructure morphologies.

Solvent control of longitudinal fibre growth

An ideal solvent dissolves the peptide in a monomeric form at high dilution, while allowing self-assembly at higher concentrations, such as upon evaporation following drop casting; that is, the solvent facilitates an equilibrium between associated and dissociated forms. It was found that the three point supramolecular H-bonding self-assembly motif is too strong for *reversible* self-assembly as irreversible fibre formation was seen in all solvents. Methanol retained a large population of the peptide in a monomeric or small oligomeric form, with only a few macrofibres forming immediately after dissolution. Aging of the solution, however, yielded more macrofibres and abundant nanofibres in the deposits, suggesting a nucleation-controlled process.

Nucleation requires that Ac-β[3][LIA] forms three parallel H-bonds that satisfy the 14-helical geometry[1]. Strong H-bonding of the solvent molecules to the amides which participate in the intermolecular H-bonds poses an activation energy barrier to both nucleation and growth. Alcohols exhibit decreasing H-bonding strength with increasing length of the alkyl chain. Thus the competition for inter-peptide H-bonding decreases from methanol to ethanol and isopropanol, resulting in faster fibre formation in isopropanol.

Only ethanol and isopropanol yielded evidence of post-deposition fibre growth in a temperature dependent manner. The dendritic hierarchical structures assembled overnight, confirming that the bulk solutions also contained a significant population of monomeric peptides and that the deposits retained a substantial amount of solvent. Given that the time would be sufficient for the solvent to evaporate from the surface, it appears that, at the temperatures investigated, the sum of H-bonding and van der Waals attraction of solvent molecules to the peptide is stronger than the thermal energy kT (k is the Boltzmann constant, T is the temperature), which is routinely used as a measure of the strength of second order interactions[19]. This "solvent entrapment" effect thus offers a method to control the kinetics of supramolecular self-assembly post deposition, and thus the density and homogeneity of the surface coverage.

Solvent control of inter-fibril interactions: geometry effects

The control of the hierarchical structure has been achieved through variation of the relative strengths of the inter-fibril interactions: solvophobic attraction, VdW attraction, and inter fibril H-bonding. Of these, H-bonding is geometrically the best defined. Inter-fibril H-bonding can impose rigidity on the superstructure, creating straight fibres and rods of a crystalline appearance. In Ac-β[3][LIA], inter-fibril H-bonding is only possible through the exposed C-terminal carboxyl group, which in crystal structures of similar β-peptidestypically binds to a carbonyl oxygen of an amide of the adjacent fibril[1], as depicted in Figure 5b. Another possibility for inter-fibril H-bonding is carboxyl dimerization (Figure 5b). In both cases, parallel and antiparallel geometries are equally feasible (Figure 5). Crystal structures suggest the prevalence of (b) in antiparallel

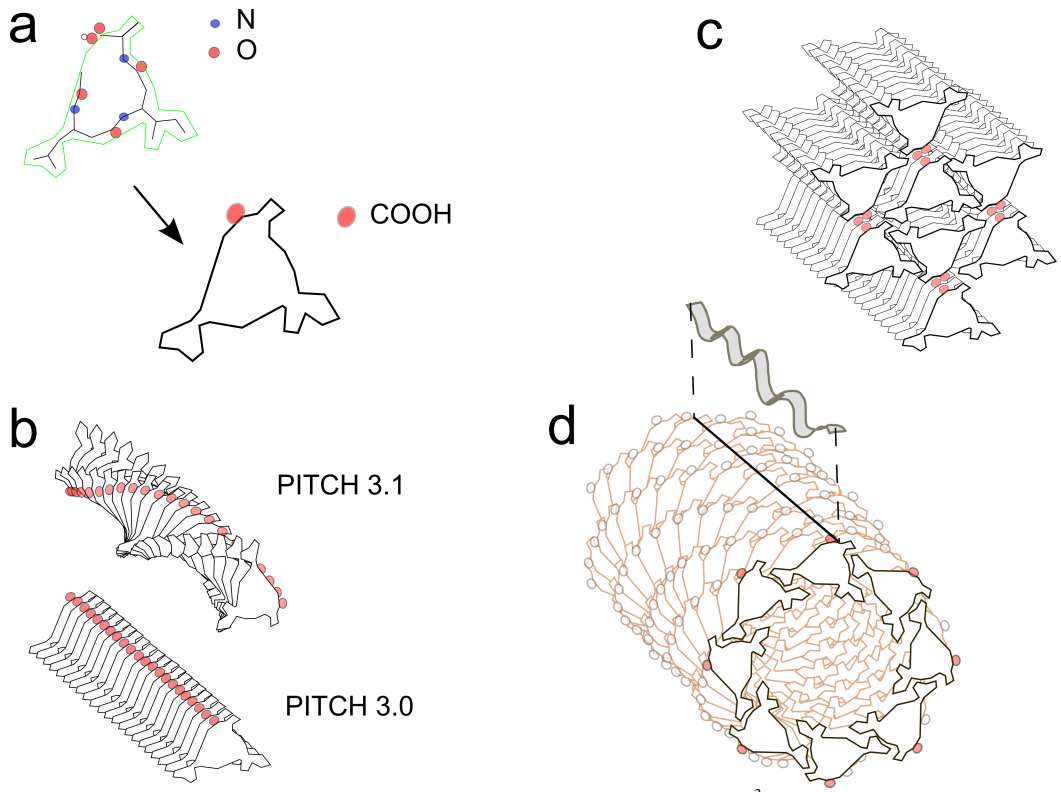

Figure 6: Schematic representation of self-assembly geometries. a, outline of helical Ac-β[3][LIA] monomer; b, two possible geometries of the helical core fibril (nanorod); c, in aprotic solvents, COOH is free; inter-fibril H-bonding isallowed with the C-terminal carboxyl; d, in protic solvents, C-terminus is solvated, leading to VdW structural optimization of fiber bundles.

geometry, however fibres are less ordered structures and thus the existence of the other three geometries cannot be ruled out.

In protic solvents H-bonding of the C terminus to the solvent may be stronger than inter-fibril H-bonding. In this case VdW and/or solvophobic interactions define the structure. VdW is a weak short distance force acting between the side chains of Ac-β[3][LIA] that is further weakened in high dielectric constant media such as water. Yet, overall VdW forces can be substantial when acting between long fibres. VdW energy minimization occurs by achieving the closest possible packing between side chains, fully utilizing local pockets of geometric compatibility and may impose complex, hierarchical structure on the self-assembled Ac-β[3][LIA].

H-bonding between solvent molecules, such as in water and alcohols, leads to the formation of an organized shell around solutes causing an apparent attraction between them. This is the solvophobic effect that is best known as hydrophobicity in water, but which is present in alcohols as well to a lesser degree[26]. The dominance of the solvophobic effect squeezes the outer envelope of the associated Ac-β[3][LIA] fibres together, prohibiting the thermal motion needed for the alignment during VdW energy minimization and thus it results in geometrically much less defined structures than the H-bonding or VdW interaction, such as soft bundles of fibres.

Figure 6 depicts the structure of the dominant self-assembly geometries. Panel A is a schematic of the outline of the Ac-β[3][LIA] in its helical form, derived from the crystal structure[1]. Inter-fibril H-bonding imposes a near-perfect pitch of three residues on the fibres (panel c), forming rigid, tightly packed, effectively crystalline structures, such as in case of chloroform solvent.

Where inter-fibril H-bonding is prohibited by C terminus-solvent interaction (as in Figure 6b), the twisting assembly with a slightly imperfect pitch results, which is closer to the 14-helix geometry[16]. The assembly can tolerate some degree of torsional strain, within 10-15 deg, allowing a VdW structural optimization of fiber bundles, with the carboxyl group (that H-bonds to the solvent) facing outwards (panel d). The resulting thick fibers interact/assemble in a twisted geometry. Importantly, the measured diameter of the smallest fibers in the AFM images in the presence of protic solvents is ~8-10 nm which is consistent with such a core structure.

Upon analysis, the dominance of the respective interactions can be identified in the images of the Ac-β[3][LIA] nanostructures. Inter-fibril H-bonding dominates in chloroform, producing straight rods and needles. In contrast, acetone solvent did not aid the formation of similar structures, as the ketone oxygen can H-bond with the C-terminal carboxyl of the peptide, suppressing the dominant H-bonding interaction, resulting in the formation of fibre bundles and radial structures. Thus inter-fibril H-bonding can be switched off by using a solvent that can H-bond to the C-terminal carboxyl.

When inter-fibril H-bonding is prohibited, the dielectric constant of the medium allows tuning between the dominance

of the VdW and the solvophobic interactions. Thus, in water, hydrophobicity dominates and bundles of fibers are formed, whereas in the alcohols, the reduction of dielectric constants from methanol to isopropanol exhibit increasing VdW effects as reflected in the geometrical complexity. The slower release of solvent in the cases of ethanol and isopropanol facilitates the surface diffusion needed to build the dendritic geometries with twisted rope-like branches which are truly hierarchical structures. Surface templating occasionally lead to the formation of 15-20 nm high flat ribbon structures, such as in the case of ethanol. This height is consistent with the size of the smallest branches of the dendritic structures. Thus ribbons are likely formed by the parallel alignment of the same fibers that form the dendritic structures, as the relatively high dielectric constant (24.2) of ethanol weakened VdW interactions, hindering but not prohibiting the formation of higher order geometries. At 37°C there were more flat ribbons than at room temperature, thus temperature aids faster solvent release which favors ribbon formation.

Conclusions

Control over superstructure morphology of the β-peptide Ac-β^3[LIA] was achieved by variation of the relative strengths of the second-order interfibril interactions by different solvents. The fibrils interact through a combination of solvophobic, VdW and H-bonding interactions, where the C-terminal carboxyl residues play a determining role. In apolar solvents where the C-terminal carboxyl residues do not interact with the solvent, inter-fibril H-bonding dominates, leading to the formation of straight fibre bundles. In alcohols, carboxyl residues are solvated and thus inter-fibril H-bonding is less prominent and a balance between solvophobic and van der Waals effects allows the formation of radial, dendritic hierarchical structures. In water, hydrophobic effects dominate over van der Waals interactions leading to the formation of rope-like hierarchically twisted structures, in effect an artificial silk-like thread. Nucleation also was successfully controlled with temperature. The ability to control the higher order self-assembled morphology is a unique feature of our peptides that offers a wide range of applications from surface modifications through to nanocomposites and smart fibers.

Experimental

Materials. Methanol, ethanol, isopropanol, chloroform and acetone of HPLC/ spectrophotometric grade were purchased from Sigma-Aldrich (Castle Hill, NSW, Australia). Ultrapure (Sartorius AG, Goettingen, Germany)) water of a resistivity of 18.2 Ωcm was used for all experiments. Ac-β^3[LIA] peptide was prepared by solid state peptide synthesis as previously described[1].

Peptide solutions were freshly prepared in methanol, isopropanol, ethanol, water, acetone and chloroform by dissolving 1 mg of Ac-β^3[LIA] peptide in 1 ml of solvent in each case. The solutions were vortexed for 3 min, and then incubated in a water bath at 50°C for ~3h.

Atomic Force Microscopy (AFM). Approximately 2µl of sample solution was deposited onto a freshly cleaved mica surface. In the case of chloroform and acetone solutions, 4 µl was needed to deposit sufficient amount of material on the surface. The samples were covered with a Petri-dish to avoid dust contamination and were allowed to dry at either room temperature (~22-24°C) or at 37°C. All samples were incubated overnight unless stated otherwise. AFM images were obtained with an Ntegra system (NT-MDT, Russia), in scan-by-sample configuration. Non-contact mode silicon AFM cantilevers (NSG30, NTMDT) with a typical spring constant of 72 Nm^{-1} and a nominal tip radius of 10 nm were used for AFM imaging. All samples were imaged in ambient conditions using semi-contact (tapping) mode at 512x512 pixel resolution and 0.5-1 Hz scan rate.

Optical microscopy. Peptide solutions were dried within the sample vial by slow evaporation of the solvent. For imaging, Nikon Eclipse TS100 inverted optical microscope was used with DS-F1 camera.

Acknowledgements

Authors acknowledge the Australian Research Council (DP1093675 and LP120200794) for financial support.

Notes and references

[a]School of Molecular Sciences, La Trobe University, Australia.
[b]Department of Biochemistry & Molecular Biology, Monash University,Australia.
[c] School of Chemistry, Monash University,Australia.

1. M. P. Del Borgo; A. I. Mechler; D. Traore; C. Forsyth; J. A. Wilce; M. C. J. Wilce; M. I. Aguilar; P. Perlmutter, *Angewandte Chemie-International Edition,* 2013, **52**, 8266.
2. S. Mann, *Nature Materials,* 2009, **8**, 781; D. N. Woolfson; Z. N. Mahmoud, *Chemical Society Reviews,* 2010, **39**, 3464; L. E. R. O'Leary; J. A. Fallas; E. L. Bakota; M. K. Kang; J. D. Hartgerink, *Nature Chemistry,* 2011, **3**, 821.
3. A. Lakshmanan; S. G. Zhang; C. A. E. Hauser, *Trends in Biotechnology,* 2012, **30**, 155.
4. J. T. Borenstein; E. J. Weinberg; B. K. Orrick; C. Sundback; M. R. Kaazempur-Mofrad; J. P. Vacanti, *Tissue Engineering,* 2007, **13**, 1837; L. Q. Wu; G. F. Payne, *Trends in Biotechnology,* 2004, **22**, 593; J. Nicolas; S. Mura; D. Brambilla; N. Mackiewicz; P. Couvreur, *Chemical Society Reviews,* 2013, **42**, 1147.
5. S. H. White; W. C. Wimley, *Annual Review of Biophysics and Biomolecular Structure,* 1999, **28**, 319; J. Venkatraman; S. C. Shankaramma; P. Balaram, *Chemical Reviews,* 2001, **101**, 3131; S. H. Gellman, *Accounts of Chemical Research,* 1998, **31**, 173; D. J. Hill; M. J. Mio; R. B. Prince; T. S. Hughes; J. S. Moore, *Chemical Reviews,* 2001, **101**, 3893.
6. S. G. Zhang, *Nature Biotechnology,* 2003, **21**, 1171.
7. H. Cui; M. J. Webber; S. I. Stupp, *Biopolymers,* 2010, **94**, 1; F. Versluis; H. R. Marsden; A. Kros, *Chemical Society Reviews,* 2010, **39**, 3434; I. W. Hamley, *Soft Matter,* 2011, **7**, 4122.
8. S. Santoso; W. Hwang; H. Hartman; S. G. Zhang, *Nano Letters,* 2002, **2**, 687.
9. H. Cui; T. Muraoka; A. G. Cheetham; S. I. Stupp, *Nano Letters,* 2009, **9**, 945; V. Castelletto; I. W. Hamley; J. Perez; L. Abezgauz; D. Danino, *Chemical Communications,* 2010, **46**, 9185.
10. J. R. Porter; T. T. Ruckh; K. C. Popat, *Biotechnology Progress,* 2009, **25**, 1539; J. K. Tessmar; A. M. Gopferich, *Advanced Drug Delivery Reviews,* 2007, **59**, 274; T. C. Holmes, *Trends in Biotechnology,* 2002, **20**, 16.
11. E. S. Place; N. D. Evans; M. M. Stevens, *Nature Materials,* 2009, **8**, 457.
12. K. Y. Lee; S. H. Yuk, *Progress in Polymer Science,* 2007, **32**, 669.

13. R. Lakes, *Nature,* 1993, **361**, 511.
14. D. H. Appella; L. A. Christianson; D. A. Klein; D. R. Powell; X. L. Huang; J. J. Barchi; S. H. Gellman, *Nature,* 1997, **387**, 381.
15. M. S. Cubberley; B. L. Iverson, *Current Opinion in Chemical Biology,* 2001, **5**, 650.
16. R. P. Cheng; S. H. Gellman; W. F. DeGrado, *Chemical Reviews,* 2001, **101**, 3219.
17. K. Rajagopal; J. P. Schneider, *Current Opinion in Structural Biology,* 2004, **14**, 480.
18. S. G. Zhang, *Biotechnology Advances,* 2002, **20**, 321.
19. J. N. Israelachvili, *intermolecular and surface force*. 1999; Vol. ISBN: 978-0- 12-375182-9 Academic Press., p xl 632.
20. A. R. Hirst; D. K. Smith, *Langmuir,* 2004, **20**, 10851.
21. J. Makarevic; M. Jokic; B. Peric; V. Tomisic; B. Kojic-Prodic; M. Zinic, *Chemistry-a European Journal,* 2001, **7**, 3328.
22. Y. L. Yang; C. Wang, *Current Opinion in Colloid & Interface Science,* 2009, **14**, 135; D. W. Bolen; I. V. Baskakov, *Journal of Molecular Biology,* 2001, **310**, 955; I. A. Sedov; B. N. Solomonov, *Journal of Structural Chemistry,* 2013, **54**, 262.
23. L. M. Greig; D. Philp, *Chemical Society Reviews,* 2001, **30**, 287; S. C. Zimmerman; F. W. Zeng; D. E. C. Reichert; S. V. Kolotuchin, *Science,* 1996, **271**, 1095.
24. S. Hwang; Q. Shao; H. Williams; C. Hilty; Y. Q. Gao, *Journal of Physical Chemistry B,* 2011, **115**, 6653; A. N. Rissanou; E. Georgilis; E. Kasotaids; A. Mitraki; V. Harmandaris, *Journal of Physical Chemistry B,* 2013, **117**, 3962; T. Arakawa; Y. Kita; J. F. Carpenter, *Pharmaceutical Research,* 1991, **8**, 285.
25. S. Ramachandran; M. B. Taraban; J. Trewhella; I. Gryczynski; Z. Gryczynski; Y. B. Yu, *Biomacromolecules,* 2010, **11**, 1502.
26. T. Yamaguchi; H. Furuhashi; T. Matsuoka; S. Koda, *Journal of Physical Chemistry B,* 2008, **112**, 16633.

